Surface Modifications of Bioglass Immersed in TRIS-Buffered Solution. A Multitechnical Spectroscopic Study

Marta Cerruti,*,† Claudia L. Bianchi,‡ Francesca Bonino,† Alessandro Damin,† Alessandra Perardi,† and Claudio Morterra†

Department of Chemistry I.F.M. and Center of Excellence NIS, University of Turin, Consortium INSTM, Research Unit of Turin University, Via P. Giuria 7, 10125 Torino, Italy, and Department of Physical Chemistry and Electrochemistry, v.Golgi 19, 20133 Milano, Italy

Received: February 9, 2005; In Final Form: May 14, 2005

Bioglass 45S5 is used in the medical field as a bone regenerative material. In fact, when immersed in body fluid, a layer of hydroxy carbonate apatite (HCA), an analogue to the mineral phase that bones are made of, is deposited on its surface. A mechanism that would explain this process has been hypothesized and includes cation leaching from the glass to the solution and formation of both a silica-rich layer and a Ca/P-rich surface layer, prior to the actual crystallization of HCA. The present paper analyzes the dissolution of 2-μm-size particles of Bioglass in TRIS-buffered solution, focusing on the modifications occurring at the surface of the particles. Results from Transmission FT-IR, Raman, and X-ray Photoelectron Spectroscopy were compared in order to obtain this information. In all cases, precise spectral band assignments were obtained by comparing Bioglass spectra, before and after reaction, with the spectra registered on some selected reference samples. The results confirm the hypothesized mechanism of Bioglass reactivity and yield new insights on the surface modifications of the samples. In particular, the following is shown: the strength of the surface H-bonding system and of water coordination decreases during the reaction; surface carbonates, initially mainly bound to Na, are substituted by an increasing amount of Ca-bound carbonates; and the final calcium phosphate layer obtained is very similar, but not identical, to carbonated hydroxyapatite.

Introduction

Bioglass is a melt-derived glass composed of 45% SiO_2, 24.5% Na_2O, 24.5% CaO, and 4% P_2O_5 (weight percentages) and is used clinically as bone-regenerative material in dental and orthopaedic applications.[1] When Bioglass is immersed in a physiological solution, a layer of hydroxycarbonate apatite (HCA), an analogue to the mineral phase that bones are made of, is deposited on its surface. Collagen fibrils are then incorporated into this layer, and a biological bond between the host bone and the glass is formed. The reaction sequence that brings about the deposition of HCA was at first hypothesized by Hench and Clark[2] and involves cation release from the glass with consequent increase of the solution pH, formation of a silica-rich layer, and precipitation of a Ca/P-rich layer that further crystallizes as HCA.

The goal of the present contribution is to validate this well-known reaction mechanism and to give some new insight into the modifications occurring at the surface of Bioglass during this process. The understanding at a nanoscale level of surface reactivity is crucial because all of the interactions with the living tissue occur in this region. We will approach the problem using three different spectroscopic techniques, that is, FTIR, Raman, and X-ray Photoelectron Spectroscopy (XPS). The results obtained with these techniques will be supported by NMR data, which will be reported in a forthcoming paper.

The literature concerning spectroscopic studies of Bioglass dissolution is vast, especially for what concerns IR spectroscopy.[3−7] Still, many important details, such as the type of surface hydroxyl and carbonate groups, have not been understood thoroughly. Moreover, peak assignments done by different authors are often contradictory, especially for Raman spectroscopy.[7−11] At last, only a few papers can be found in the literature concerning, for this type of systems, the detailed analysis of XPS peak components[12−14] because the use of XPS has been limited mainly to a surface elemental survey.[15,16] For this reason, a comparison between the results obtained with Bioglass and with a number of reference systems turned out to be necessary in order to get to an accurate and reliable spectral band assignment.

FT-IR transmission spectroscopy was carried out on pure sample pellets (i.e., not diluted with KBr) so that the bands relative to surface groups were intense enough to be observed. The formation of a phosphate-rich layer was followed with Raman spectroscopy because the vibrations of PO groups are far more Raman-intense than those of SiO groups, unlike what was observed with IR spectroscopy. A survey of the amount of atomic species present at the surface of Bioglass before and after reaction was obtained with XPS. Moreover, changes occurring in the structure of C, O, Si, and P surroundings were studied by peak-resolving the relevant XPS bands.

In the past, most of the research concerning Bioglass was carried out on bulk pieces or rough powders.[17−20] In our study, we will use small particles of Bioglass instead (with a diameter of $\sim$2 μm), following a more recent research trend.[3,4,21] Smaller particles seem to have promising potential applications;[22−24] for example, studies completed recently have shown that these particulates can be effective in reducing gingival inflammation.[25]

* Corresponding author. E-mail: martacerruti@yahoo.com.
† Department of Chemistry I.F.M. and Center of Excellence NIS.
‡ Department of Physical Chemistry and Electrochemistry.

10.1021/jp050705t CCC: $30.25
Published on Web 07/08/2005

TABLE 1: Nominal Surface Composition (mol %) of Reference Doped Silica Samples

doped silica sample	SiO_2	Na_2O	CaO	P_2O_5
A200/Na	80	20		
A200/Ca*X*	100−*X*		*X*	
A200/P	97			3
A200/CaP	73		24	3

We will study the reactivity of Bioglass in a simple TRIS-buffered solution at pH 8[2,26,27] instead of a more complex simulated body fluid (SBF).[28] This was decided in order to analyze the dissolution and reprecipitation processes involving Bioglass alone, without the presence in solution of high concentrations of Ca, P, and other ions that could precipitate easily in the presence of just a few nucleation sites. Recent works showed that this approach can give useful results.[29,30]

Materials and Methods

Materials. Bioglass powders, with an average particle size of ~2 μm and ~90 μm and a high-area sol−gel bioactive glass termed 58S (containing 60 mol % SiO_2, 36% CaO, and 4% P_2O_5) were supplied kindly by NovaMin Technology Inc., Alachua, Florida. These materials will be referred to as 4502, 4590, and 58S, respectively. A sol−gel synthesized glass, composed of 60 mol % SiO_2 and 40% CaO and used for comparison, was supplied by Dr. R. J. Newport (School of Physical Sciences, The University of Canterbury, UK) and will be referred to as S60C40. Reference samples of $CaCO_3$ and Na_2CO_3 were purchased from Merck. Samples of hydroxyapatite (HA) and hydroxycarbonate apatite (HCA) were supplied kindly by the National Research Center (ISTEC-CNR) of Faenza, Italy. The reference pure silica that was analyzed was the amorphous nonporous Aerosil A200 (Degussa, Frankfurt A. M., Germany), obtained by flame pyrolysis of $SiCl_4$. Doped silica systems were obtained by impregnating A200 silica with the "incipient wetness" method, which allows the introduction of all of the dopant species at the surface of the samples. Titrated aqueous solutions were used in amounts just sufficient to wet, but not overwet, all of the A200 powder, and then the samples were oven dried at ~373 K for ~30 min. Solutions used to obtain Na-, Ca-, and P-doped samples were prepared using $NaHCO_3$, $Ca(NO_3)_2$, and H_3PO_4, respectively. The Na- and Ca-doped silica powders were treated further in air at 873 K for 2 h to decompose and eliminate nitrates and carbonates, respectively. The doped silica samples will be referred to as A200/Na, A200/Ca*X* (where *X* stands for the mol % of Ca introduced), and A200/P. A portion of the A200/Ca26 powder was impregnated further with a dosed amount of H_3PO_4 to obtain a sample doped with both Ca and P that will be referred to as A200/CaP.

The surface composition of all of the doped silica samples is reported in Table 1.

IR Spectroscopy. For IR measurements, the powders were compressed in the form of self-supporting pellets of ~10 mg cm^{-2}. All of the spectra were obtained with a FTIR Spectrometer (Bruker IFS 113v, equipped with a MCT cryodetector). The homemade quartz infrared cell, equipped with KBr windows, was connected to a conventional vacuum line (residual pressure $\approx 10^{-5}$ Torr) and allowed to perform in strictly in situ conditions both thermal treatments on the sample pellets and probe molecules adsorption/desorption cycles on the activated samples. All of the IR spectra were recorded at beam temperature (BT), that is, the temperature reached by (white) sample pellets in the IR beam. The BT is estimated to be some 30 K higher than the actual room temperature (RT).

Raman Spectroscopy. Raman measurements have been performed by employing a 244-nm laser line (as generated by the Coherent Innova 300C MotoFred Frequency-Doubled Ion Laser System) and a Renishaw Micro-Raman System 1000 shaped to work with three different lines: (i) 244 nm (40 984 cm^{-1}), (ii) 325 nm (30 770 cm^{-1}), and (iii) 442 nm (22 625 cm^{-1}). The photons scattered by the sample were dispersed by a grating monochromator (3600 L/mm) and collected simultaneously on a CCD camera. The power at the sample was less than 25% of the output power at the laser head (about 30 mW) so that samples turned out to be stable under the laser beam. The collection optic was a ×15 objective, optimized for UV light. Spectra were recorded in air.

X-ray Photoelectron Spectroscopy. XPS measurements were performed with an M-Probe Instrument (SSI) equipped with a monochromatic Al Kα source (1486.6 eV) with a spot size of 200 × 750 μm^2 and a pass energy of 25 eV, providing a resolution of 0.74 eV. The energy scale was calibrated with reference to the $4f_{7/2}$ level of a freshly evaporated gold sample, at 84,00 ± 0,1 eV, and with reference to the $2p_{3/2}$ and 3s levels of copper at 932,47 ± 0,1 and 122,39 ± 0,15 eV, respectively. With a monochromatic source, an electron flood gun was used to compensate the buildup of positive charge on the insulating samples during the analyses: a value of 10 eV was selected to perform measurements on these samples. For all of the samples, the C_{1s} peak level was taken as internal reference at 284.6 eV. The accuracy of the reported binding energies (BE) is approximately ±0.2 eV. The quantitative data were also checked accurately and reproduced several times, and the error due to uncertainty in spectral deconvolution is estimated to be as low as ±1%.

Results and Discussion

FTIR Results. The IR spectra of Bioglass 4502 before and after immersion in TRIS-buffered solutions are shown in Figure 1. All of the spectra have been recorded after a vacuum treatment of the samples at BT for ~40 min. Attention should be paid when comparing the IR spectra of different samples because IR band intensities depend on many parameters, including pellet (optical) thickness. For this reason, one or more bands that are known to remain constant in intensity with treatments are usually used as an internal standard in order to make meaningful comparisons. But in the present case there are no bands that can be used for this purpose because the Bioglass structure changes completely during dissolution in TRIS. So, even though the starting pellet thickness was kept as constant as possible when preparing the samples for IR analysis, it should be recalled that a real quantitative analysis is not feasible on the basis of IR spectra alone.

The most relevant spectral features observed in Figure 1 and their major changes in the course of the reaction are summarized in Table 2. It is quite evident that, as long as the reaction proceeds, some significant changes in surface hydroxylation and carbonation occur (see the bands at ~3740−3500 cm^{-1} and at ~1490−1420 cm^{-1}, respectively) and a silica-rich layer is formed (see the intensity of the overtone/combination bands at ~1980 and ~1870 cm^{-1}).

The red shift of the band relative to the δ_{HOH} mode of molecular water (from ~1660 cm^{-1} on the starting sample to ~1640 cm^{-1} after reaction, a rather large shift for a sensitive vibrational mode) would indicate that the strength of water coordination at the surface and the strength of the relevant H-bonding system decrease when samples are reacted. Still, in that frequency range some overtones of more intense low-ν

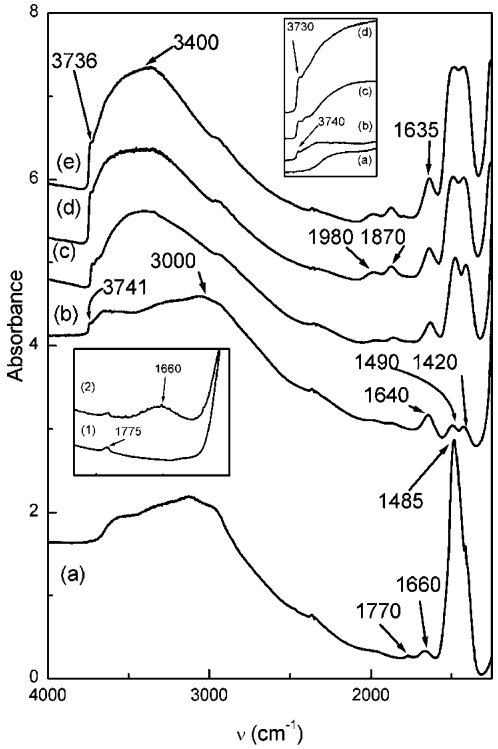

Figure 1. IR spectra of samples outgassed at BT for 40 min: 4502 as received (a) and after 1 h (b), 6 h (c), 1 day (d), and 1 week (e) of reaction in TRIS. Upper inset: blown-up segment in the ν_{OH} frequency region of 4502 as received (a) and after 1h (b), 6 h (c), and 1 week (e) of reaction in TRIS. Lower inset: the 1850−1500 cm^{-1} frequency range of 4502 as received, vacuum treated at 473 K for 1 h (1), and then put in contact with ∼20 Torr water (2).

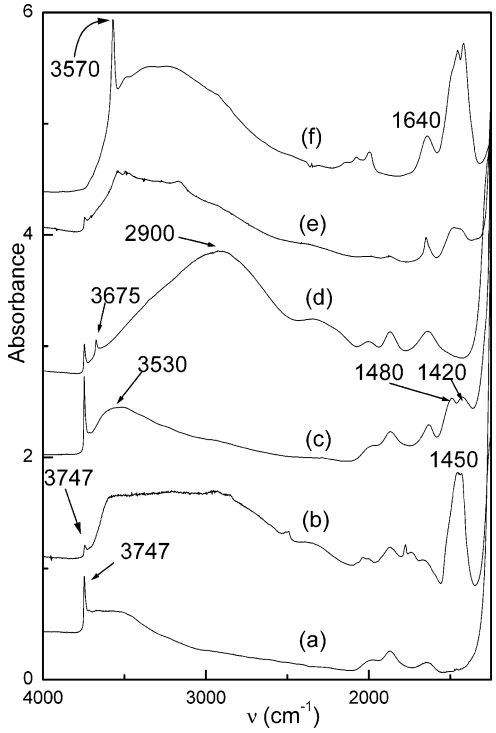

Figure 2. IR spectra of reference samples outgassed at BT for 40 min: A200 (a), A200/Na (b), A200/Ca10 (c), A200/P (d), A200/CaP (e), HA (f).

bands are often found (for example, silicate or carbonate bands). To determine if the band observed in spectrum a is really related to coordinated water, we vacuum treated a 4502 sample at 473 K and then put it in contact with water vapor. The spectra relative to this experiment are shown in the lower inset of Figure 1: the ∼1660 cm^{-1} band disappears when 4502 is dehydrated (spectrum 1) and reappears at the same frequency when water is allowed on it (spectrum 2). This undoubtedly allows one to assign the band at ∼1660 cm^{-1} to the δ_{HOH} mode of coordinated water. Analogue results were obtained after vacuum treating at 473 K and rehydrating the samples reacted in TRIS solution (spectra not shown for brevity): after rehydration, the δ_{HOH} band always reappeared at the same frequency first observed in Figure 1 before the dehydration step. The red shift of the δ_{HOH} band from ∼1660 cm^{-1} to ∼1640 cm^{-1} is then a real indication of a net decrease in the strength of water coordination at the surface of the reacted samples.

A comparison with some reference samples seemed necessary in order to better understand the evolution of hydroxylation and carbonation during 4502 dissolution in TRIS (Figure 1). In Figure 2, the spectra of A200, A200/Na, A200/Ca10, and A200/CaP are shown (spectra a−e) together with HA (spectrum f). In Table 3, hydroxyls and surface carbonates found on these samples are compared. For a more detailed analysis of some of these samples, see Cerruti et al.[31,32]

The hydroxyl band observed on the 4502 sample as received, and still after 1 h of reaction (spectra a and b in Figure 1), presents a relative maximum at a very low frequency (∼3000

TABLE 2: Most Important Spectral Features of Figure 1

band position (cm^{-1})	assignment	evolution
3750−2500	ν_{OH} (free and H-bonded hydroxyl groups)[41−44]	On the starting sample, there are no components at ν > 3710 cm^{-1}, and the apparent maximum of the H-bonded hydroxyl group band (that spreads from ∼3700 to ∼2500 cm^{-1}) is located at ∼3000 cm^{-1}. After 1 h reaction, a peak at ∼3740 cm^{-1} appears, relative to free SiOH groups, and moves to ∼3730 cm^{-1} after 6 h of reaction. The apparent maximum of the H-bonded hydroxyls band shifts to ∼3400 cm^{-1} after 6 h of reaction.
1980, 1870, and, partly, 1680	combination and overtone bands of SiO vibrations[44]	Bands well visible after ∼6 h of reaction. Increase and remain constant after 1 day of reaction.
1770	overtone band of CO vibrations[34]	Present only on the starting 4502 sample.
1640−1660	δ_{HOH} deformation mode (coordinated water)	Red-shifts when passing from the starting sample to the reacted ones. Increases in the course of the reaction.
1490−1410	ν_{CO} stretching mode(s) (surface carbonates)[34]	The starting sample shows only one intense band at ∼1485 cm^{-1}. This band disappears in the earliest stages of immersion and is replaced by a band with two components ($\Delta\nu \approx 70$ cm^{-1}), which increases in intensity in the course of the reaction.

TABLE 3: Comparison between Hydroxyl Groups and (Surface) Carbonate Groups on the Reference Samples of Figure 2

species	pure silica	ion-doped silica samples	HA
Hydroxyl groups	Sharp peak at ~3747 cm^{-1} (free SiOH groups). Low intensity band at 3700−3000 cm^{-1} (H-bond interacting SiOH groups. No coordinated water is present on pure SiO_2).	The band of H-bonded OH-bearing species (hydroxyls and coordinated water) increases in intensity. On A200/P, a peak at 3670 cm^{-1} is observed (POH groups[45]), and the apparent maximum of the band relative to interacting hydroxyls is shifted to lower ν. Doping with both P and an excess of Ca (A200/CaP) cancels out the effects produced by P alone.	Sharp and intense peak at ~3570 cm^{-1} because of structural CaOH groups.[46] Intense band of interacting hydroxyls, centered at ~3300 cm^{-1}.
Surface carbonates	Absent	A peak is present at ~1450 cm^{-1}, only slightly split, on Na-doped silica. Two bands at ~1480 and ~1420 cm^{-1} are visible on Ca-doped silica. The extent of band splitting is related to the asymmetry of surface carbonate structures: the lower the splitting, the higher the symmetry (no splitting at all would be present in purely ionic carbonates of D_{3h} symmetry).[34,37,47]	Complex band at ~1410−1490 cm^{-1}. Carbonates observed on this sample are just surface carbonates, formed by contact with air. They are supposed to be different from the bulk carbonates that would be found in HCA.[46]

cm^{-1}; $\Delta\nu_{OH} \approx -750$ cm^{-1}) and is indicative of the presence at the surface of a strong H-bonding system.[33] This OH spectral pattern is comparable not only to the hydroxyl band found on A200/P (Figure 2d) but also to that observed on A200/Na (Figure 2b), especially for what concerns the "double maximum" aspect of the H-bonded OH band envelope (with apparent maxima at ~3600 and ~2900 cm^{-1}, respectively).

After 6 h of reaction (Figure 1c), the apparent maximum of the band of H-bonded OH-bearing species becomes unique and shifts to a higher frequency so that the overall band becomes more similar to that observed on A200/Ca10 (Figure 2c), even if in reacted 4502 the free silanol band at ~3740 cm^{-1} remains quite weak. This is thought to be indicative of the emerging of Ca at the surface: a surface excess of Ca hinders the effects of surface Na and/or P, as observed, for instance, on the silica system doped with both P and an excess of Ca (Figure 2e). The formation, after 1 h of reaction, of a small peak at ~3740 cm^{-1} (Figure 1b) is indicative of the formation of a small amount of free surface silanols (compare with the spectrum of pure silica, Figure 2a). The frequency shift from ~3740 to ~3730 cm^{-1} observed after 2 days of reaction seems to indicate an increase in the amount of H-bonded surface species, that is, it probably means that the newly formed silica-rich layer is strongly hydrated.

The one-peak band relative to carbonates observed on the starting 4502 sample (spectrum 1a) is similar to the virtually unsplitted carbonate peak present on A200/Na (spectrum 2b), whereas the double band that is formed with increasing intensity after immersion in TRIS buffer is very similar to the carbonate absorption found on A200/Ca10 (spectrum 2c). This is again an indication of the emerging of Ca surface cations that carbonates can bind to, whereas the virtually total elimination of carbonates bound to Na is in agreement with a fast release of Na in solution, as reported in the literature.[4,15] The band of carbonates observed after one week of reaction (spectrum 1e) is, as expected, very strong. Its shape turns out to be quite different from the complex carbonate band formed on HA or on HCA (spectrum not shown, because the carbonate zone is virtually identical to that of HA, even though on HA carbonation is due only to air exposure). Instead, the carbonate band of 4502 reacted for one week in TRIS solution (1e) is more similar to that of carbonates formed on A200/Ca (2c).

Raman Results. *Choice of the Laser*. Raman spectra of 4502 as received and reacted in TRIS buffer solution are reported in Figure 3. The spectra of the main section of the figure have been collected using a laser exciting line at 244 nm because fluorescence was observed if higher wavelengths were used. The presence of fluorescence is a source of big troubles in Raman spectroscopy because some peaks can be hidden by the high baseline scattering and the relative intensity of peaks can be modified artificially by the presence of spectral oscillations. An example of this problem is shown in the top right inset of Figure 3, where 4502 spectra recorded with the 244-nm laser line (spectrum 1) and the 442-nm laser line (spectrum 2) are compared. Spectrum 2 clearly shows both high scattering of the baseline and some oscillations centered at ~1620 and ~1385 cm^{-1}. These oscillations also continue in the spectrum at lower wavenumbers and artificially increase the intensity of a tiny real band centered at ~860 cm^{-1}.

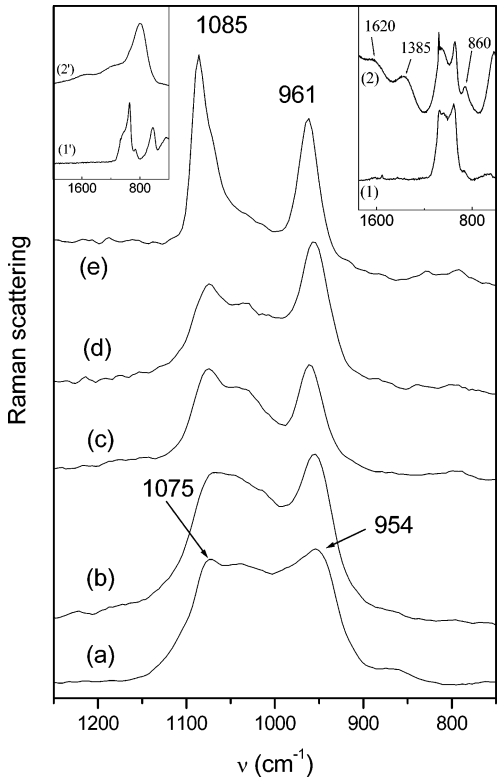

Figure 3. Raman spectra of 4502 as received (a), and after 1h (b), 6 h (c), 1 d (d), and one week (e) of reaction in TRIS buffer. Upper right inset: Raman spectra of 4502 collected with laser line at 244 nm (1) and 442 nm (2). Upper left inset: Raman spectra of different particle size samples of Bioglass collected with laser line at 1064 nm: 4590 (1′) and 4502 (2′).

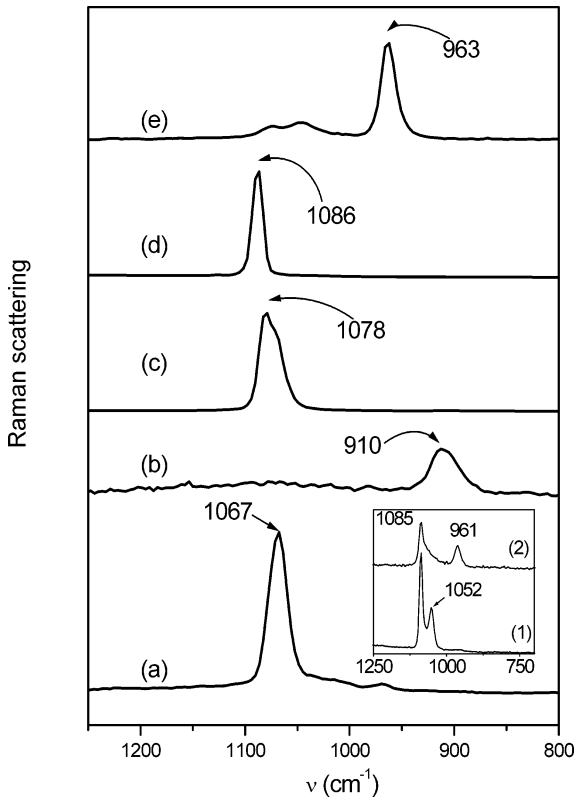

Figure 4. Raman spectra of some reference samples: A200/Na (a), A200/P (b), Na_2CO_3 (c), $CaCO_3$ (d), HA (e). The inset reports the spectra of the sol−gel synthesized samples S60C40 (1) and 58S (2).

It is interesting that less fluorescence was detected using a higher frequency laser, whereas usually lower frequency lasers are used specifically to avoid fluorescence problems. We believe that, in the present case, the small particle size of the Bioglass sample somehow affects the fluorescence properties of the material. In fact, we also tried to measure the spectra of Bioglass samples of different average particle size using a near-IR laser line. The spectra are shown in the top left inset of Figure 3: spectrum 1′ refers to 90-μm particles (4590), and spectrum 2′ refers to 2-μm particles (4502). An increasing amount of fluorescence was observed when analyzing smaller particles. Still, even if the relative intensities can be different, the spectral position of the main peaks present in the spectrum of 4502 measured with the UV laser (see spectrum 3a) is similar to that observed in the spectra of 4590 and measured with the near-IR laser, both by us (spectrum 1′, top left inset of Figure 3) and in the literature.[21]

Sample Analysis. In the 1250−800 cm^{-1} spectral zone, where the most relevant spectral features were observed, sample 4502 as received presents a complex band with relative maxima at ∼1075 and ∼954 cm^{-1}. During reaction in TRIS, the broad central component of this band (∼1050 cm^{-1}) is eroded gradually and, after one week of reaction (spectrum 3e), only two sharp peaks are visible at ∼1085 and ∼960 cm^{-1}. The peak at ∼960 cm^{-1} has been found by many researchers who analyzed the formation of an HCA layer on samples similar to Bioglass and has been assigned to the ν_{PO} mode of apatite.[9−11] A peak at a frequency similar to our 1085 cm^{-1} band has also been observed and has been related to both the asymmetric stretching vibration of PO_4^{3-} groups[9,10] and a ν_{CO} mode of carbonates.[7,11]

To better understand the nature of these bands, and the overall spectral evolution, some reference samples were analyzed (Figure 4). By comparison with the spectra of Na_2CO_3 (Figure 4c) and $CaCO_3$ (Figure 4d), we can confidently assign the higher frequency components of the complex band observed in spectrum 3a of the 4502 sample to the symmetric ν_{CO} vibration (the ν_1 mode) of Na and Ca ionic carbonates. The peak of the ν_1 mode in $CaCO_3$ (4d) is sharp, symmetric, and centered at 1086 cm^{-1}. This frequency is reported as typical of both calcite and aragonite structures.[34] The peak of the ν_1 mode of solid Na_2CO_3, centered at ∼1078 cm^{-1} (spectrum 4c), presents a shoulder at lower frequency, possibly because of the presence of two sites with slightly different symmetry for carbonate ions.[35] The ν_1 mode of Na_2CO_3 in aqueous solution (not shown; see Martinez et al.[35]) is a single symmetric peak at 1067 cm^{-1}, that is, at the same frequency observed in the reference A200/Na system, shown in spectrum 4a.

The lowest frequency component of spectrum 3a of the 4502 system is located at ∼954−961 cm^{-1} and can be assigned to a ν_{PO} mode of phosphate groups surrounded by different atomic configurations. This can be understood by analyzing the spectra of the following samples. (i) A200/P (Figure 4b): the doping of silica with P induces the formation of a broad peak at ∼910 cm^{-1} (note that no relevant peaks are present in the Raman spectrum of pure A200); (ii) sol−gel synthesized glasses 58S and S60C40 (inset of Figure 4): these glasses have in their composition very similar percentages of SiO_2 and CaO, but the S60C40 system does not contain P_2O_5, whereas the 58S system does (see the Materials and Methods section). Both spectra show a twin peak with a maximum at ∼1085−1050 cm^{-1}, but in the spectrum of 58S (spectrum 2) there is an additional and well-resolved peak located at ∼961 cm^{-1}, ascribable to the presence of P; (iii) HA (Figure 4e): the ν_1 mode of PO_4^{3-} groups falls at ∼963 cm^{-1}, as also reported in the literature.[36]

The broad and mostly unresolved central part of the complex band present at ∼1000−1050 cm^{-1} in the spectrum of 4502 can be related to the stretching of SiO^-Na^+ groups, as can be understood by comparing the spectrum of 4502 reacted in TRIS for one week (Figure 3e) with that of the sol−gel glass 58S (spectrum 2 in the inset of Figure 4), which does not contain Na. The two spectra are virtually identical: this suggests that the bands that decreased in intensity and eventually disappeared during 4502 reaction were related to Na and that after one week of reaction, (virtually) no Na is present on the surface of 4502.

After one week of reaction, only the peak relative to ν_{PO} at ∼961 cm^{-1}, and that relative to ν_{CO} at ∼1085 cm^{-1}, with a shoulder at 1070 cm^{-1}, are visible. Then, Raman spectroscopy is clearly indicating the formation, on the surface of reacted 4502, of a layer of carbonated hydroxyapatite. The carbonation observed here is not completely comparable to that of HCA: in HCA, the ν_{CO} mode of type A carbonates would fall at ∼1100 cm^{-1}, and that of type B carbonates would fall at ∼1070 cm^{-1}.[36] We can thus conclude that carbonates formed on 4502 after one week of TRIS reaction are mostly in a configuration similar to that of $CaCO_3$ (Figure 4d) and only partially similar to type B carbonates of HCA.

TABLE 4: Bulk and Surface Atomic Percent Composition of 4502[a]

atomic %	O	Si	Ca	Na	P	C
4502 bulk	40.1	21.5	19.2	18.1	1.1	
4502 surface	35.4	10.5	4.3	17.1	0.8	29.7
4502 surface (recalculated without C)	52.6	15	6.2	25.2	1	

[a] Surface composition was obtained with XPS survey. (Explored with the XPS approach, "surface" means the outermost 40−50 Å layer).

XPS Results. The surface composition of 4502 as received was analyzed by XPS, and the results are shown in the third

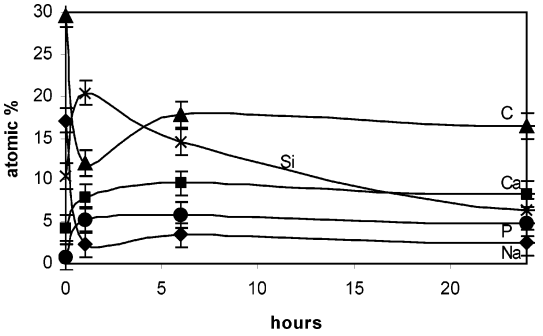

Figure 5. XPS analysis of surface composition changes of 4502 immersed in TRIS-buffered solution: atomic percentages of C (▲), Ca (■), Si (×), P (●), and Na (◆).

line of Table 4. In the second line of Table 4, bulk composition expressed in atomic percentage is reported. A first remarkable difference is that a lot of C is found on the surface of 4502, and this can be due to both hydrocarbonaceous impurities, that very often contaminate samples surface, and some specific surface C (due, for instance, to surface carbonates). The resolution of the C peak can help in discriminating these components, as will be shown below. To make a possibly more reasonable comparison between surface and bulk composition, surface composition has also been calculated after eliminating the C component. The results, shown in the fourth line of Table 4, do not seem to change much with respect to those shown on the third line, at least for what concerns the relative amounts of the various elements. Either way, more Na is visible on the surface, and less Ca and Si, as compared to the bulk composition, whereas the presence of P in the bulk and on the surface is very similar. The higher surface Na/Ca ratio can be due to different factors: for example, migration from bulk to the surface during glass formation (fusion) and/or during shelf-aging, easier breaking of $SiO^{-}Na^{+}$ bonds rather than $SiO^{-}Ca^{2+}$ bonds during grinding.

Changes of surface composition occurring during the first hours of dissolution in TRIS buffer are reported in Figure 5. The following hours of reaction have also been analyzed (up to one week), but the results are not shown because the main changes turn out to occur in the first few hours. After that, the trends of the various elements follow those outlined in Figure 5. Na decreases drastically in the first hour and then remains nearly constant (this is in agreement with both the increase of Na measured in solution[15] and with what was hypothesized in the previous paragraphs on the basis of Raman and FTIR results). C decreases first, and then increases, matching the trend observed with FTIR spectroscopy for surface carbonates (see

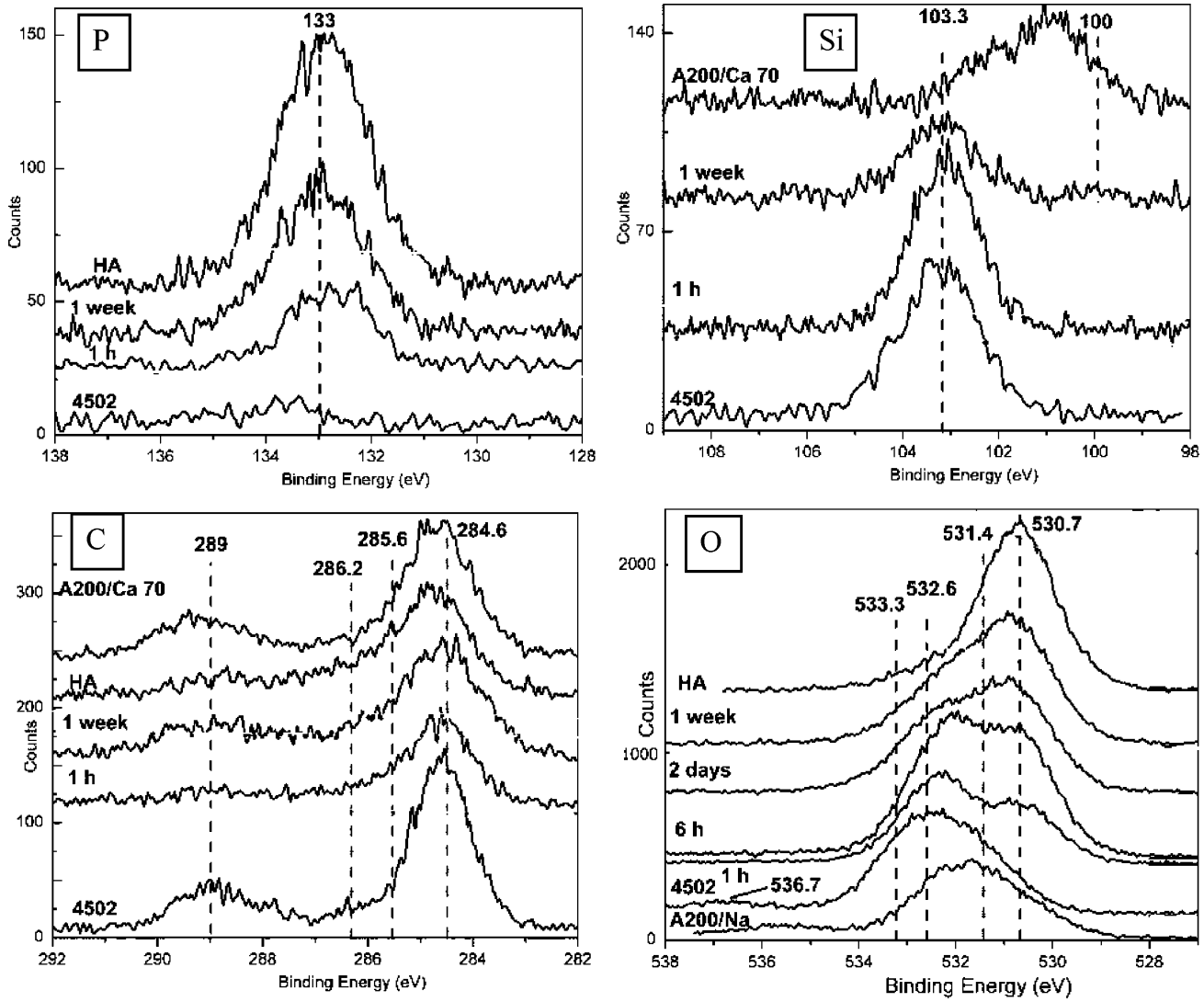

Figure 6. XPS spectra for 4502 before and after reaction, and for some reference samples, as indicated on the curves in the various sections. The four regions correspond to the binding energies of P, Si, C, and O.

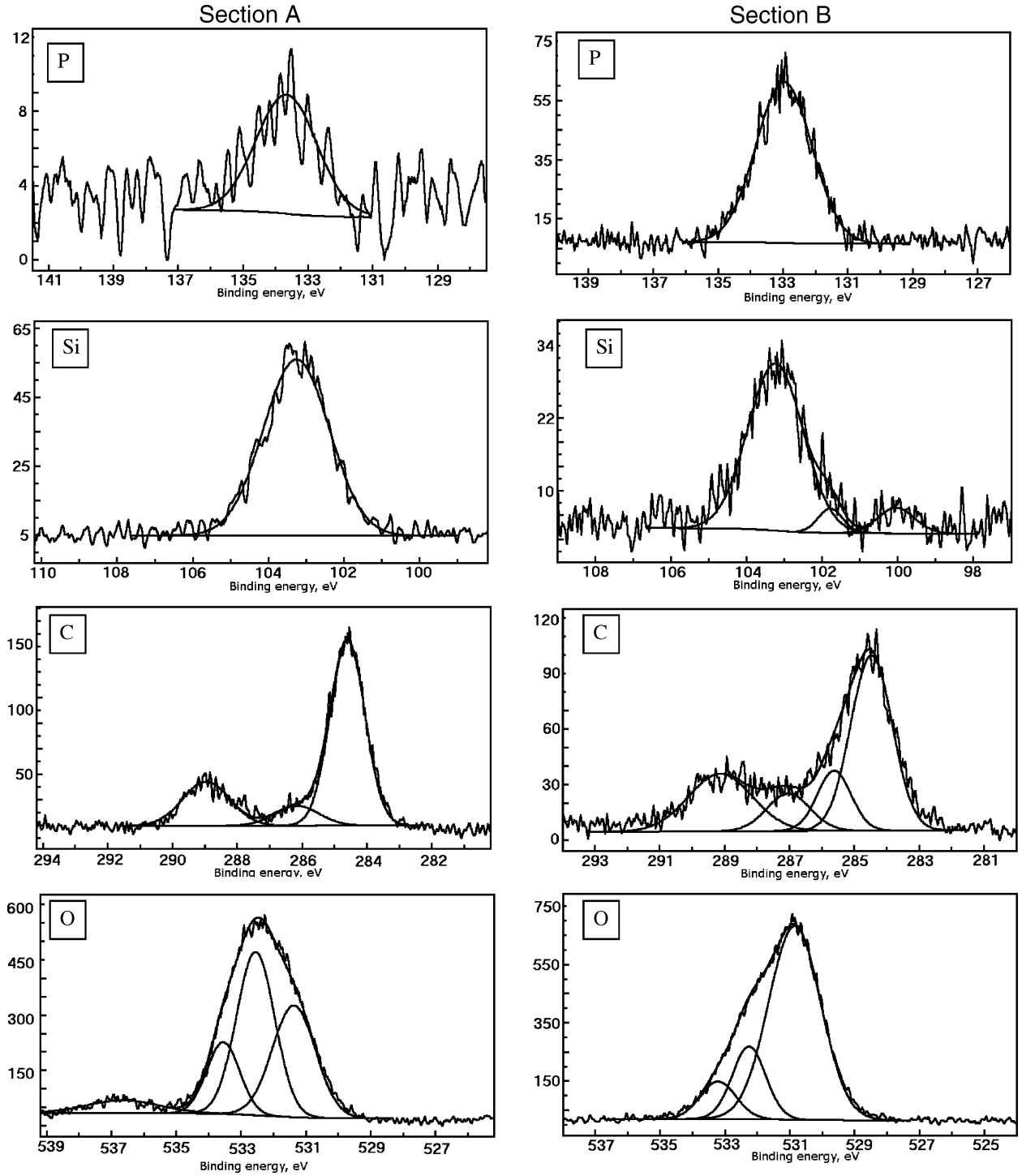

Figure 7. Peak analysis of XPS spectra of 4502 before reaction (section A) and after 1 week of reaction in TRIS (section B). The spectral regions corresponding to P, Si, C, and O have been analyzed, as reported on the graphs.

the spectral pattern in Figure 1). Si increases in the first hour and then decreases, whereas Ca and P increase first and then remain (almost) constant. This confirms the hypothesized formation of a silica-rich layer in the first period of reaction, then covered by a layer of calcium phosphate(s).

Figure 6 shows the spectral evolution of the peaks relative to P, Si, C, and O of 4502 before and after reaction, compared with the spectra of some reference samples. The main components of the peaks are indicated in the figure, to facilitate the reading. A more detailed peak analysis for both 4502 and reference samples is shown in Figures 7 and 8. The assignment of the various spectral components is summarized in Table 5.

Based on these data, changes in the structure of P, Si, C, and O surroundings can be depicted as follows.

(i) P Peak. The position of the P peak does not change much before and after reaction in TRIS. Mostly, the P peak increases in intensity as the reaction proceeds, and after one week it is centered at the same energy of the phosphate peak found on HA (compare section 7B,P with section 8B,e). In this case, sample A200P is not a good reference for XPS analysis because its P spectrum shows a partly resolved component at higher energy (see 8A,a) because of the formation of pyrophosphate structures. These structures are broken by the presence of an excess Ca^{2+}, as shown by the spectrum of A200CaP (inset of

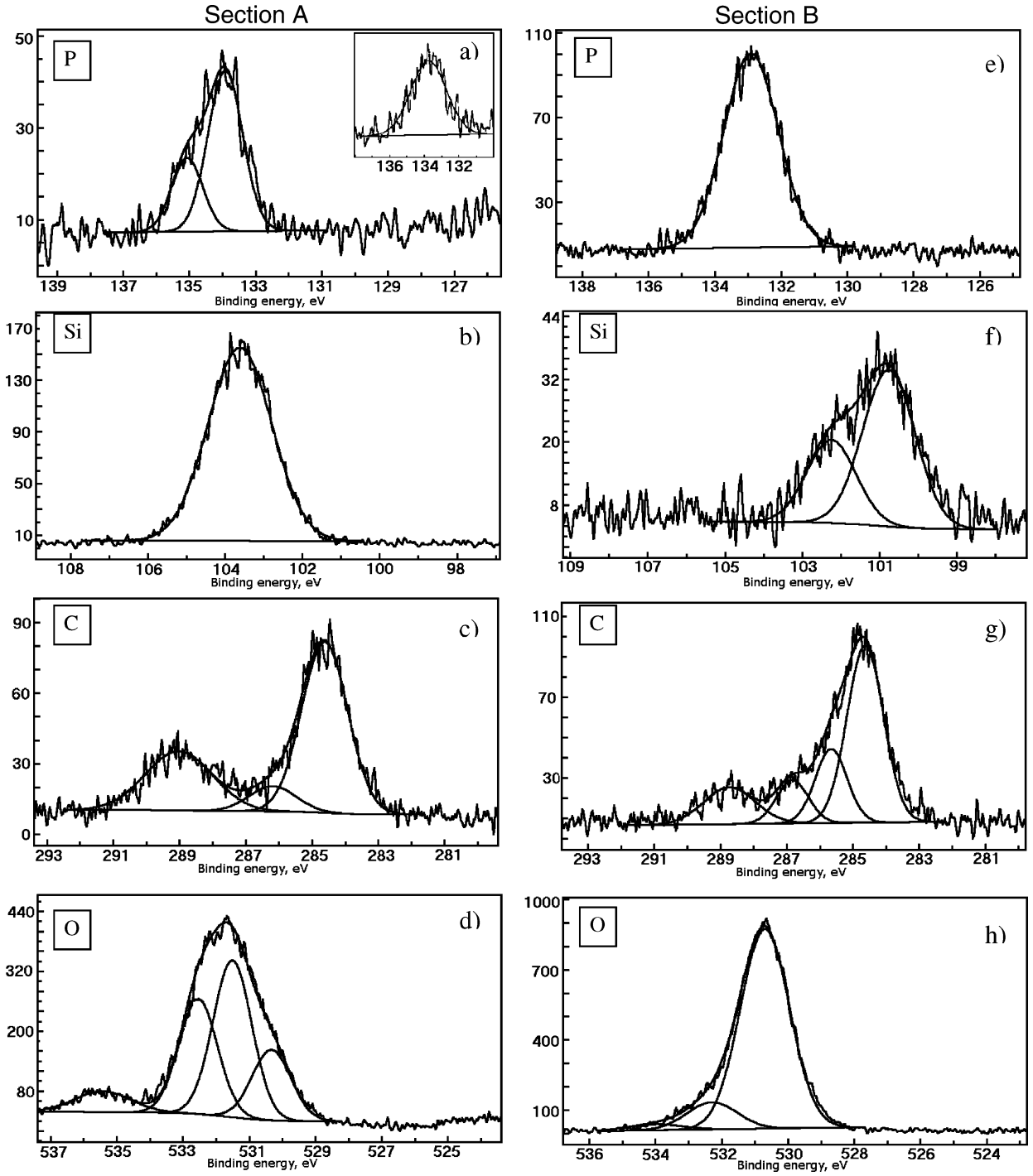

Figure 8. XPS peak analysis of selected reference samples, similar to 4502 before reaction (Section A) and after 1 week of reaction (Section B). The spectral regions corresponding to P, Si, C, and O have been analyzed, as reported on the graphs. The spectra refer to: A200/P (a), A200CaP (inset of section a), A200 (b), A200/Na (c and d), HA (e, g and h), and A200/Ca70 (f).

Figure 8A,a): the component at high energy disappears, and a single peak, centered at an energy similar to that of both 4502 and HA, is observed.

(ii) Si Peak. On the starting 4502 sample only one component is found for Si, centered at an energy similar to that observed on the plain silica A200 (compare section 7A,Si with section 8A,b). This peak remains in the same position up to one week of reaction, when new components, centered at lower energies, start being observed (section 7B,Si). Such low-energy components are also observed on A200/CaX oxidic systems (e.g., see spectrum 8B,f) in which the higher the doping, the lower the energy of the new Si peak components. This could mean that a mixed Si−Ca oxidic phase is formed, possibly because of the sinking of some Ca ions into the silica-rich layer that was shown above to form on 4502 after a few hours of reaction. The low-energy components are thought to be indicative of the presence of non bridging oxygen(s) in the Si coordination sphere, as mentioned in Table 5.

(iii) C Peak. The evolution of the C peak is quite complex. On both bioactive glasses and reference systems, hydrocarbonaceous contamination is found constantly, characterized by the lowest energy component at ∼284.6 eV. (Note that a hydrocarbonaceous contamination is often also observed in the 3000−2900 cm^{-1} region of the background IR spectra of all systems, as soon as the decreased intensity of the band of H-bonded OH species allows the detection of tiny ν_{CH} vibrational modes; for

TABLE 5: Peak Resolution and Assignment of XPS Bands[a]

peak	component	relevant spectra where the component is found	assignment[b]
P	~133 eV	HA, A200CaP, 4502 after reaction; on 4502 as received and on A200/P at 133.7 and 133.9 eV, respectively	PO_4-like phosphate groups
	~135 eV	A200/P	P_2O_7 and P_4O_{10}-like pyrophosphate structures
Si	multiple components at lower energies (102.2−100.04 eV)	4502 reacted for one week, and A200/Ca*X*	SiO^- structures (where not all of the oxygens are bridging ones)[12]
	~103.6 eV	A200 on 4502 before and after reaction at ~103.3 eV	SiO_2 bulk structure
C	~284.6 eV	4502 before and after reaction; HA	hydrocarbonaceous contaminants
	~285.6 eV	4502 after reaction; HA	C−O groups
	~286.2 eV	4502 before and after reaction; HA	C═O groups
	>287 eV	4502 before and after reaction; HA, A200/Na, A200/Ca*X*	CO_3^{2-} groups
O	~530.7 eV	HA, 4502 after reaction	PO_4^{3-}
	~531.4 eV	HA, 4502 as received	CO_3^{2-} (e.g., $CaCO_3$) in 4502 as received it could also be related to SiO^- groups[12,48]
	~532.6 eV	A200, 4502 before and after reaction	SiO_2
	~533.3 eV	HA; ~533.6 eV on 4502 before and after reaction	OH^-
	>533.6 eV	HA, 4502 as received	H_2O

[a] See Figures 6−8. [b] A reference for all of these assignments is Moulder et al.[49] Some more specific references are listed in the Table.

example, see spectra 1c−e and 2b). On the starting 4502 sample, only three main C components can be observed (Figure 7A,C), whereas on all of the reacted samples four components are present (Figure 7B,C). A three-component spectrum is also observed on reference samples A200Ca70 (Figure 6, section C) and A200Na (Figure 8A,c), whereas the four-component band is very similar to that found on the HA sample (Figure 8B,g). Carbon spectral components observed at energies between ~285.6 and ~286.8 eV are usually assigned, in order of increasing energy, to C−O and C═O bonds. In the present case, the C−O and C═O bands may be related to some sort of surface carbonate complexes. In fact, it is known that on oxidic surfaces carbonates are not always completely ionic, but can also have single and double CO bonds depending on the structure and/or symmetry they have when bound to the surface.[37] The highest-energy C component is to be related to ionic carbonates, as demonstrated by its preminent intensity in the nearly two-component spectrum of A200/Na (Figure 8Ac). The intensity of this high-energy component decreases drastically when passing from the starting 4502 sample to the one reacted in TRIS for 1 h (see the first two spectra in Figure 6, section C) and then increases again as the dissolution proceeds. After one week of reaction, the spectral position of this component is ~289.1 eV, that is, higher than the figure (~288.7 eV) found on HA (spectrum 8B,g) or HCA (spectrum not shown) and more similar to that observed on the A200/Ca70 system (see the top spectrum in Figure 6, section C). This means that the ionic carbonate structure formed on the Ca phosphate layer deposited on the reacted 4502 glass is not (yet) completely coincident with that of the carbonates formed on HA and somehow still feels the presence of the silica matrix in which it is embedded.

(iv) O Peak. Also, the evolution of the O1s peak is quite complex and difficult to analyze because some components can be assigned to more than one species. On the starting 4502 sample (at least) four components can be found (see Figure 7A,O). On the basis of widely agreed literature reference data,[38,39,40] the very broad band at highest energy (~536.6 eV) is ascribed to undissociated coordinated water. The second component, at ~533.5 eV, may be related to OH groups, and the third one, at 532.5 eV, is indicative of the presence of regular SiO_2 (i.e., of O atoms covalently shared by two [SiO_4] tetrahedra). The lowest-energy component, at ~531.4 eV, can be ascribed to both carbonates and SiO^- groups (see also the description in Table 5).

When 4502 is immersed in TRIS, the lowest energy component shifts to ~530.7 eV (Figure 7B,O), a binding energy similar to that of the O1s peak of phosphate groups in HA. During the dissolution in TRIS, the intensity of this component increases, whereas the intensity of the component at ~532.5 eV, relative to regular SiO_2, suddenly decreases after 6 h of reaction. This is another indication of the formation of an increasingly thick layer of Ca phosphate, which after a few hours of reaction gradually covers the silica-rich layer. A similar trend was observed in SBF for the O1s peak by Takadama et al.;[14] in that case, though, the changes were slower because the starting material was only a Na-silicate glass, which is less bioactive than Bioglass.

The component at high energy, relative to coordinated molecular water, disappears after immersion in TRIS buffer and is never recovered. A similar band is also observed (and only) on the A200/Na (see spectrum 8Ad) reference system. This indicates that only on the starting 4502 sample and on A200/Na could some coordinated water resist the ultrahigh vacuum conditions used when carrying out XPS analysis. This is a neat confirmation of what hypothesized previously on the basis of the red shift of the δ_{HOH} peak in IR spectra of 4502 before and after reaction (Figure 1, spectra a and b): at the surface of sample 4502 as received, the strength of water coordination is higher than that on the reacted samples because of the abundant presence of Na. When 4502 reacts, its surface Na concentration is depleted and, even though with FTIR we observe an increasing overall amount of water bound to the surface of 4502 (possibly due to an increase of surface area), with XPS we observe the presence of coordinated water only on the starting 4502 sample because only a fraction of more strongly bound water can be measured in UHV conditions.

Conclusions

Surface modifications occurring on Bioglass during dissolution in TRIS buffered solution at pH 8 were analyzed with IR,

Raman, and X-ray photoelectron spectroscopy. A parallel study of a number of reference samples was carried out in order to obtain a precise spectral band assignment.

The general mechanism proposed in the literature in order to explain the formation of HCA on a Bioglass surface that involves glass dissolution and formation of a silica-rich layer, which is later covered by a calcium-phosphate-rich layer, was confirmed by all of the techniques. Still, some new insight came out of the comparison of the results obtained.

The well-known Na depletion from the glass to the solution was shown to be connected with a transformation of surface carbonates: Na-coordinated carbonates are dominant at the surface of Bioglass as received, whereas after immersion in TRIS these were eliminated and substituted by an increasing amount of Ca-coordinated carbonates. Both IR and XPS showed that the final type of carbonates obtained was not exactly analogous to the carbonates found on the surface of hydroxyapatite but were more similar to $CaCO_3$ or to carbonates formed on a Ca-doped silica. The formation after one week of reaction of a silica structure contaminated with Ca ions was also shown by the XPS analysis of Si surrounding.

The formation of a phosphate-rich layer was shown to be connected to a change in the structure of P surrounding in the glass by both Raman spectroscopy and XPS. In particular, on Bioglass as received, both phosphate and pyrophosphate groups were observed with XPS, in a configuration similar to that of a P-doped silica. After a few hours of dissolution, only phosphate groups analogous to the ones observed in HA were found.

The presence of Na at the surface of Bioglass as received not only determines the type of surface carbonation but also increases the strength of surface H-bonding interactions (as observed with FTIR spectroscopy) and of molecular water coordination (as shown by the fact that only on 4502 and on A200/Na some coordinated water could be observed when the samples were analyzed in the ultrahigh vacuum conditions necessary for XPS).

Acknowledgment. This research was financed partly with funds of the Italian Ministry MIUR (Project COFIN2003, Prot. 2003032158), and of the Center of Excellence for Nanostructured Interfaces and Surfaces (University of Turin). Samples of bioactive glass 58S and of Bioglass 45S5 were supplied kindly by NovaMin Technology Inc., Alachua, Florida. We thank Dr. L. Bertinetti (University of Turin) for the execution of the IR spectra of hydroxyapatite and for fruitful discussions.

References and Notes

(1) Hench, L. L.; Splinter, R. J.; Allen, W. C.; Greenlee, T. K. *J. Biomed. Mater. Res. Symp.* **1971**, *2*, 117.

(2) Clark, A. E.; Hench, L. L. *J. Biomed. Mater. Res.* **1976**, *10*, 161.

(3) Jones, J. R.; Sepulveda, P.; Hench, L. L. *J. Biomed. Mater. Res. (Appl. Biomater.)* **2001**, *58*, 720.

(4) Sepulveda, P.; Jones, J. R.; Hench, L. L. *J. Biomed. Mater. Res*. **2002**, *61*, 301.

(5) Peitl, O.; Dutra Zanotto, E.; Hench, L. L. *J. Non-Cryst. Solids* **2001**, *292*, 115.

(6) ElBatal, H. A.; Azooz, M. A.; Khalil, E. M. A.; Soltan Monem, A.; Hamdy, Y. M. *Mater. Chem. Phys*. **2003**, *80*, 599.

(7) Rehman, I.; Karsh, M.; Hench, L. L.; Bonfield, W. *J. Biomed. Mater. Res.* **2000**, *50*, 97.

(8) Gonzalez, P.; Serra, J.; Liste, S.; Chiussi, S.; Leon, B.; Perez-Amor, M. *J. Non-Cryst. Solids* **2003**, *320*, 92.

(9) Notingher, I.; Boccaccini, A. R.; Jones, J.; Maquet, V.; Hench, L. L. *Mater. Charact.* **2003**, *49*, 255.

(10) Rehman, I.; Hench, L. L.; Bonfield, W.; Smith, R. *Biomaterials* **1994**, *15*, 865.

(11) Rehman, I.; Smith, R.; Hench, L. L.; Bonfield, W. *Bioceramics* **1994**, *7*, 79.

(12) Serra, J.; Gonzalez, P.; Liste, S.; Serra, C.; Chiussi, S.; Leon, B.; Perez-Amor, M.; Ylanen, H. O.; Hupa, M. *J. Non-Cryst. Solids* **2003**, *332*, 20.

(13) Vallet-Regi, M.; Perez-Pariente, J.; Izquierdo-Barba, I.; Salinas, A. J. *Chem. Mater.* **2000**, *12*, 3770.

(14) Takadama, H.; Kim, H.-M.; Kokubo, T.; Nakamura, T. *J. Am. Ceram. Soc.* **2002**, *85*, 1933.

(15) Perez-Pariente, J.; Balas, F.; Vallet-Regi, M. *Chem. Mater.* **2000**, *12*, 750.

(16) Polzonetti, G.; Iucci, G.; Frontini, A.; Infante, G.; Furlani, C.; Avigliano, L.; Del Principe, D.; Palumbo, G.; Rosato, N. *Biomaterials* **2000**, *21*, 1531.

(17) Pereira, M. M.; Clark A. E.; Hench L. L. *J. Biomed. Mater. Res.* **1994**, *28*, 693.

(18) Nakamura, T.; Yamamuro, T.; Higashi, S.; Kokubo, T.; Ito, S. *J. Biomed. Mater. Res.* **1985**, *19*, 685.

(19) Hench, L. L. *J. Am. Ceram. Soc*. **1991**, *74*, 1487.

(20) Andersson, O. H.; Kangasniemi, I. *J. Biomed. Mater. Res.* **1991**, *25*, 1019.

(21) Sepulveda, P.; Jones, J. R.; Hench, L. L. *J. Biomed. Mater. Res. (Appl. Biomat.)* **2001**, *58*, 734.

(22) Stoor, P.; Soderling, E.; Salonen, J. I. *Acta Odontol. Scand.* **1998**, *56*, 161.

(23) Allan, I.; Newman, H.; Wilson, M. *Biomaterials* **2001**, *22*, 1683.

(24) Rectenwald, J. E.; Minter, R. M.; Rosenberg, J. J.; Caines, G. C.; Lee, S.; Moldawer, L. L. *Shock* **2002**, *17*, 135.

(25) Tai, B. J.; Du, M. Q.; Jiang, H.; Zhong, J. P.; Greenspan, D. C.; Clark, A. E. *J. Dent. Res. A* **2004**, *83*, 1545.

(26) Clark, A. E.; Pantano, C. G.; Hench, L. L. *J. Am. Ceram. Soc.* **1976**, *59*, 37.

(27) Hench, L. L. *Fundamental Aspects of Biocompatibility*; CRC Press: Boca Raton, FL, 1981; Vol. 1, p 67.

(28) Kokubo, T.; Kushitani, H.; Sakka, S.; Kitsugi, T.; Yamamuro, T. *J. Biomed. Mater. Res.* **1990**, *24*, 721.

(29) Cerruti, M.; Greenspan, D.; Powers, K. *Biomaterials* **2005**, *26*, 1665−1674.

(30) Cerruti, M.; Greenspan, D.; Powers, K. *Biomaterials* **2005**, *26*, 4903−4911.

(31) Cerruti, M.; Magnacca, G.; Bolis, V.; Morterra, C. *J. Mater. Chem.* **2003**, *13*, 1279.

(32) Cerruti, M.; Bolis, V.; Magnacca, G.; Morterra, C. *Phys. Chem. Chem. Phys.* **2004**, *6*, 2468.

(33) Cerruti, M.; Morterra, C.; Ugliengo, P. *J. Mater. Chem.* **2004**, *14*, 3364−3369.

(34) Nakamoto, K. *Infrared and Raman Spectra of Inorganic and Coordination Compounds*; John Wiley & Sons: New York, 1986; p 87.

(35) Martinez, I.; Sanchez-Valle, C.; Daniel, I.; Reynard, B. *Chem. Geol.* **2004**, *207*, 47.

(36) Penel, G.; Leroy, G.; Rey, C.; Bres, E. *Calcif. Tissue. Int.* **1998**, *63*, 475.

(37) Busca, G.; Lorenzelli, V. *Mater. Chem*. **1982**, *7*, 89.

(38) Lim, A. S.; Atrens, A. *Appl. Phys. A* **1990**, *51*, 411.

(39) Beccaria, A A. M.; Poggi, G.; Castello, G. *Br. Corros. J.* **1995**, *30*, 283.

(40) Stypula, B.; Stoch, J. *Corros. Sci.* **1994**, *36*, 2159.

(41) Little, C. H. *Infrared Spectra of Adsorbed Species*; Academic Press: London, 1966.

(42) Davydov, V. Y. *Adsorption on Silica Surfaces*, Marcel Dekker Inc: New York, 2000; p 63.

(43) Icenhower, J. P.; Dove, P. M. *Adsorption on Silica Surfaces*; Marcel Dekker Inc: New York, 2000; p 343.

(44) Burneau, A.; Gallas, J. P. *The Surface Properties of Silicas*. John Wiley & Sons: New York, 1999; p 147.

(45) Morrow, B. A.; Lang, S. J.; Gay, I. D. *Langmuir* **1994**, *10*, 756.

(46) Rehman, I.; Bonfield, W. *J. Mater. Sci. Mater. Med.* **1997**, *8*, 1.

(47) Cerruti, M.; Morterra, C. *Langmuir* **2004**, *20*, 6382.

(48) Sprenger, D.; Bach, H.; Meisel, W.; Gutlich, P. *J. Non-Cryst. Solids* **1990**, *126*, 111.

(49) Moulder, J. F.; Stickle, W. F.; Sobol, P. E.; Bomben, K. D. *Handbook of X-ray Photoelectron Spectroscopy*; Physical Electronics Inc: Chanhassen, MN.